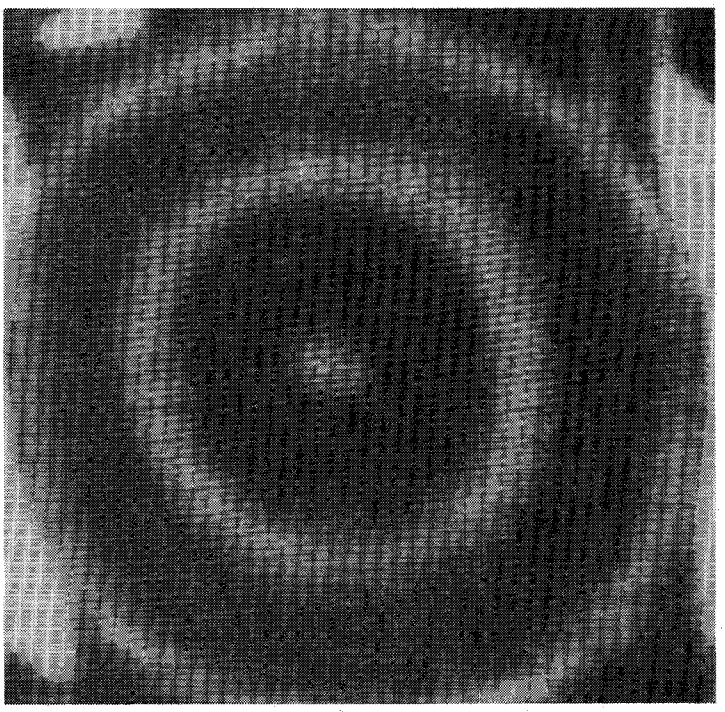

Fig. 4. Same as Fig. 3, but for a $TE_{0,2}$ mode. The two dark rings are blue to blue-green and indicate the peaks in the radiation. The light rings are yellow, and indicate nulls.[3]

where all the field components have time dependence of the form

$$e^{im\theta + ik_z z - i\omega t}$$

where k_z is the axial wavenumber, ω is the angular frequency, t is the time, and θ is the angle. In Fig. 2, we see the radial dependence of power flux for two modes ($TE_{0,2}$, $TE_{0,4}$).

$TE_{0,4}$ has four peaks between the center and the inner wall of the waveguide, while the $TE_{0,2}$ has two. It is therefore expected that the two modes will have four and two concentric rings on the field map, as is clearly visible in Fig. 3 and 4, respectively. Different modes can be identified using the same arrangement and technique—for example $TE_{2,4}$ and $TE_{12,1}$ have been identified. Also, asymmetry in the mode can be detected.

The Thomson–CSF gyrotron is designed to oscillate in the TE_{02} mode with a magnetic field of about 13.5 kG. Fig. 4 shows the pattern corresponding to this mode in the correct conditions. At a lower field, the tubes often oscillate in the $TE_{2,2}$ mode, theoretically with a rotating field pattern. The $TE_{0,n}$ modes are certainly the easiest to identify, as they are not degenerate except with TM modes that are very difficult to excite in gyrotrons.

The power flux needed to create a clear, high-quality image on the liquid crystal at (35 GHz) is on the order of 700 mW/cm^2. Of course, only a very small fraction of that power is absorbed in the liquid crystal sheet. (Based on the liquid crystal sheet material, it is estimated that only about 10^{-3} of the electromagnetic energy flux is absorbed at 35 GHz.)

References

[1] S. Ramo, J. R. Whinnery, and T. VanDuzer, *Fields and Waves in Communications*. New York: Wiley, 1965, p. 434.

[2] K. J. Kim, M. E. Read, J. M. Baird, K. R. Chu, A. Drobot, J. L. Vomvorides, A Ganguly, D. Dialetes, and V. L. Granatstein, "Design considerations for a megawatt CW gyrotron," *Int. J. Electron.*, vol. 51, pp. 427–446, Oct. 1981.

[3] G. Mourier, G. Boucher, Ph. Boulanger, P. Charbit, G. Faillon, A. Hersovici, and E. Kammerer, "A gyrotron study program," presented at *IEEE Int. Conf. on Infrared and Millimeter Waves* (Miami Beach, FL), Dec. 7–12, 1981; also, in *Infrared and Millimeter Waves*, vol. 9. New York: Academic Press, to be published.

[4] Y. Carmel, K. R. Chu, D. Dialetes, A. Fliflet, M. E. Read, K. J. Kim, B. Arfin, and V. L. Granatstein, "Mode competition, suppression and efficiency enhancement in overmoded gyrotron oscillators," *Int. J. Infrared and Millimeter Waves*, vol. 3, pp. 645–665, Sept. 1982.

[5] D. S. Levinson and R. L. Selven, "Power measurements in multimode waveguide," *Microwave J.*, vol. 10, pp. 59–64, Oct. 1967.

[6] O. F. Hinckelmann, R. L. Sleven, and L. F. Moses, "Instrumentation for the measurement of spurious emissions in waveguide," *IRE Trans. Electromagn. Compat.*, vol. EMC-6, pp. 30–37, Oct. 1964.

[7] H. E. Stockman and B. Zarwyn, "Optical film sensors for RF holography," *Proc. IEEE*, vol. 56, p. 273, Apr. 1968.

[8] C. F. Augustine, "Field detector works in real time," *Electron.*, vol. 41, pp. 118–122, June 1968.

[9] J. Pughaubert, "Visualisation des ondes électromagnetiques hyperfréquences à l'aide de cristaux liquides," *L'onde Electrique*, vol. 52, pp. 213–217, May 1972.

[10] N. P. Kerweis and J. F. McIlvenna, "Liquid crystal diagnostic techniques an antenna design aid," *Microwave J.*, vol. 20, pp. 47–49, Oct. 1977.

[3] Color photographs may be obtained by contacting one of the authors (M.E. Read).

Waveguide Modes Via an Integral Equation Leading to a Linear Matrix Eigenvalue Problem

GIUSEPPE CONCIAURO, MARCO BRESSAN, AND CINZIA ZUFFADA

***Abstract*—A numerical method for determining the modes of a rectangular or a circular waveguide strongly perturbed by axial cylindrical conduct-**

Manuscript received August 16, 1983; revised April 11, 1984. This work was supported by the Ministero della Pubblica Istruzione.

The authors are with the Dipartimento di Elettronica dell'Universitá di Pavia, 27100 Pavia, Italy.

ing objects is presented. The method is based upon an integral equation which leads to a matrix eigenvalue problem by using the Galerkin procedure. Cutoff wavenumbers are simultaneously calculated with very good precision for a number of modes near to the order of the matrix eigenvalue problem. Excellent results are obtained also when the perturbed waveguide section exhibits reentrant parts or edges. Computing time is short and storage requirements are moderate. The method is also applicable for waveguides of arbitrary cross section.

I. Introduction

The calculation of the modal fields of a uniform, hollow conducting waveguide and of their corresponding cutoff wavenumbers is equivalent to the determination of the resonant modes and frequencies of a two-dimensional resonator. Several numerical techniques have been set up in the last decades for this purpose. A comprehensive bibliography up to 1974 is given in [1] and some further algorithms and developments are described in [2]–[6].

Most of these techniques may be grouped into two classes. The former consists of techniques based upon the finite-element (difference) method or the transmission-line-matrix method which leads to either large-size standard eigenvalue matrix problems or multistep iterative schemes. The latter consists of techniques based upon the solution of integral equations by algorithms such as the method of moments, the null-field method, the point-matching method, or the auxiliary source method, which lead to the solution of small-size nonalgebraic eigenvalue problems.

The techniques belonging to the former class require *ad hoc* wise choice of the location, the shape, and the number of meshes inside the cross section of the waveguide, particularly when irregular and pointed boundaries are dealt with; moreover, their application requires time-consuming procedures and/or large computer memory availability. Storage requirements are strongly reduced for the techniques belonging to the other class, though computational time is still fairly long (especially when many modes must be computed), due to their feature of finding cutoff frequencies as zeros (or minima) of the determinant of a matrix whose elements are trascendental functions of the frequency. One of the most widely known methods belonging to this class is that described by Spielman and Harrington [7], who expressly point out that one of the main limitations of their method is the long computation time required for the calculation of the cutoff frequencies for higher order modes.

In this paper, we discuss a new algorithm which, though based on the solution of an integral equation, leads to a small-size linear matrix eigenvalue problem. This permits us to avoid the time-consuming procedure for the search of the cutoff frequencies required by other integral equation methods. The basic feature of our approach is the use of a real kernel given by recently determined forms of the dyadic Green's function for two-dimensional circular and rectangular resonators [8] instead of the commonly used free-space Green's function. These forms include rapidly converging series whose terms are rational functions of the frequency. These series may be approximated by a small number of terms without a significant loss of accuracy, so that the kernel reduces to a real rational function of the frequency, a feature which allows us to cast the problem into the form of a linear eigenvalue matrix problem.

We consider structures obtained by perturbing a circular or a rectangular waveguide of section S_0 with one (or several) axial cylindrical conducting sheet, whose intersection with S_0 is a line (or a set of lines) σ as shown in Fig. 1. This line is defined by the parametric equation

$$s = s(l)$$

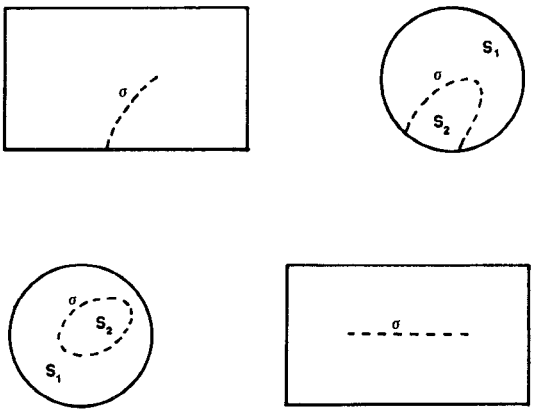

Fig. 1. Rectangular and circular waveguides perturbed by conducting sheets.

where s denotes a point on σ and l is a suitable abscissa taken on the line. Line σ may consist of separate portions, even if, for a simple illustration, in most of the following we refer to it as to a simple line. For the sake of simplicity we assume that σ has no branch points.

The electric field at a generic observation point $\boldsymbol{r}$ inside S_0 may be represented as

$$\boldsymbol{E}(\boldsymbol{r}) = -j\eta k \oint_{\sigma} \overline{\boldsymbol{G}}_e(\boldsymbol{r}, \boldsymbol{s}', k) \cdot \boldsymbol{J}_\sigma(l')\, dl' \tag{1}$$

where $s' = s(l')$ indicates a source point on σ, $k = \omega\sqrt{\epsilon\mu}$, $\eta = \sqrt{\mu/\epsilon}$, $\overline{\boldsymbol{G}}_e$ is the two-dimensional dyadic Green's function of the electric type for the two-dimensional resonator of cross section S_0, $\boldsymbol{J}_\sigma$ is the current density on the sheet, and the dash in the symbol of integral denotes the principal value. This specification is necessary when $\boldsymbol{r}$ lies on σ due to the singularity of $\overline{\boldsymbol{G}}_e$, as discussed by Yaghjian [10]. It is noted that (1) may be deduced from Yaghjian's general expression for the two-dimensional case, provided a slit-shaped principal surface element is assumed and considering that $\boldsymbol{J}_\sigma$ is tangential to σ. Due to the nature of the Green's functions we use, the field given by (1) satisfies the boundary condition on the outer circular or rectangular contour. Then, an integral equation for $\boldsymbol{J}_\sigma$ is set up simply by imposing that the tangential component of $\boldsymbol{E}$ must vanish on σ. This equation has nontrivial solutions, provided k is a resonant wavenumber of the perturbed structure, i.e., a cutoff wavenumber for a mode of the perturbed waveguide.

When σ divides S_0 into separate regions (such as S_1 and S_2 in Fig. 1(b),(c)) our method yields the modes associated with the different regions at the same time. When only one of these regions is of interest, the pertaining modes can be easily identified.

It is pointed out that, in many practical cases, waveguide shapes are actually modifications of the rectangular or the circular one. For instance, ridged waveguides such as the one recently considered by Dasgupta and Saha [3] may be regarded as a perturbed rectangular waveguide. In these cases, our approach is particularly appropriate because the unknown function $\boldsymbol{J}_\sigma$ must be determined at the perturbing surface only instead of at the entire boundary, as it is the case in other integral equation methods. This is very advantageous because it permits one to consider smaller matrices in numerical computations. Anyway, any boundary shape may be considered by inscribing a suitable tubular sheet inside a rectangular or circular contour. Also in this general case, our method permits to save computing time.

II. Fundamental Equations

The general expression for the dyadic $\bar{G}_e$ given in [8] for the rectangular and circular cross section is

$$\bar{G}_e(r,r',k)=\bar{G}_{et}(r,r',k)+z_0z_0G_{ezz}(r,r',k) \tag{2}$$

where z_0 is the unit vector directed as the waveguide axis, $\bar{G}_{et}$ is a dyadic transverse to z_0, given by

$$\bar{G}_{et}(r,r',k)=-\frac{1}{k^2}\nabla\nabla' g(r,r')+\bar{G}_{st}(r,r')+\sum_m \frac{k^2}{k_m^2\left(k_m^2-k^2\right)}e_m(r)e_m(r') \tag{3}$$

and

$$G_{ezz}(r,r',k)=g(r,r')+\sum_m \frac{k^2}{k_m'^2\left(k_m'^2-k^2\right)}\psi_m(r)\psi_m(r') \tag{4}$$

where

- r and r' generic observation and source points inside S_0, respectively;
- g the scalar two-dimensional Green's function for the two-dimensional Poisson equation subject to the condition $g=0$ at the boundary of S_0;
- k_m and k_m' the cutoff wavenumbers for the TE and TM modes, respectively, of the rectangular or circular waveguide;
- e_m the electric field for the mth TE mode;
- ψ_m the axial electric field for the mth TM mode;
- $\bar{G}_{st}$ the solenoidal dyadic, normal to the boundary, satisfying

$$\nabla\times\nabla\times\bar{G}_{st}(r,r')=\bar{I}_t\delta(r-r')+\nabla\delta' g(r,r') \tag{5}$$

where $\bar{I}_t$ is the transverse unit dyadic and $\delta(r-r')$ represents the two-dimensional delta function.

Both g and $\bar{G}_{st}$ exhibit a logarithmic singularity when r and r' coalesce. In case of a circular cross section, g and $\bar{G}_{st}$ are known in closed form. In case of a rectangular cross section, they are known in the form of a rapidly converging one-index series where the logarithmic singularity explicitly appears in the first term. For ease of reference, the expressions for g and $\bar{G}_{st}$ are given in Appendix I.

The series appearing in (3) and (4) are regular everywhere inside S_0 and converge rapidly since their terms go to zero like k_m^{-4} (or $k_m'^{-4}$). Modal functions e_m and ψ_m, which are real and normalized according to

$$\int_{S_0} e_m\cdot e_m\,ds=1$$

$$\int_{S_0}\psi_m^2\,ds=1$$

as well as the expressions for k_m and k_m', may be found in many text books (see [9], for instance).

The current density may be split into a transverse and a longitudinal component according to

$$J_\sigma(l')=J_t(l')t(l')+J_z(l')z_0$$

where t represents the unit vector tangent to σ and J_t, J_z are functions to be determined. Substituting (2)–(4) into (1), it is found that the transverse and longitudinal components of the electric field are related to J_t and J_z, respectively, via the expressions

$$E_t(r)=j\frac{\eta}{k}\int_\sigma\nabla\frac{\partial g(r,s')}{\partial l'}J_t(l')\,dl'-j\eta k\int_\sigma\bar{G}_{st}(r,s')\cdot t(l')J_t(l')\,dl'-j\eta k^3\sum_m\frac{e_m(r)}{k_m^2\left(k_m^2-k^2\right)}\int_\sigma e_m(s')\cdot t(l')J_t(l')\,dl' \tag{6}$$

$$E_z(r)=-j\eta k\int_\sigma g(r,s')J_z(l')\,dl'-j\eta k^3\sum_m\frac{\psi_m(r)}{k_m'^2\left(k_m'^2-k^2\right)}\int_\sigma\psi_m(s')J_z(l')\,dl'. \tag{7}$$

The symbol of principal value has been retained only in the first integral in (6) because the functions in the remaining integrals are regular or have an integrable singularity. For the purpose of numerical computation, it is convenient to transform the principal-value integral in (6) using the identity

$$\int_\sigma\frac{\partial g(r,s')}{\partial l'}J_t(l')\,dl'=-\int_\sigma g(r,s')\frac{\partial J_t(l')}{\partial l'}\,dl'$$

which is obtained integrating by parts, observing that the singularity of g is integrable, and taking into account the following properties of g and J_t: a) g is zero at any extremum of σ lying on the boundary of S_0; b) J_t vanishes at any extremum of σ coincident with an edge (e.g., at the tip of the fin in Fig. 1(a)).

Equation (6) is suitable for representing the field of TE modes at cutoff, in which case both the current and the electric field are transverse; (7) is suitable when treating TM modes at cutoff, in which case both the electric field and the current are longitudinal. By imposing the boundary conditions $E_t\cdot t=0, E_z=0$ on σ we obtain the following equations:

TE Modes

$$\frac{1}{k^2}\frac{\partial}{\partial l}\int_\sigma g(s,s')\frac{\partial J_t(l')}{\partial l'}\,dl'+\int_\sigma t(l)\cdot\bar{G}_{st}(s,s')\cdot t(l')J_t(l')\,dl'+\sum_m\frac{t(l)\cdot e_m(s)}{k_m^2}a_m=0 \tag{8a}$$

$$a_m=\frac{k^2}{k_m^2-k^2}\int_\sigma e_m(s')\cdot t(l')J_t(l')\,dl'. \tag{8b}$$

TM Modes

$$\int_\sigma g(s,s')J_z(l')\,dl'+\sum_m\frac{\psi_m(s)}{k_m'^2}a_m'=0 \tag{9a}$$

$$a_m'=\frac{k^2}{k_m'^2-k^2}\int_\sigma\psi_m(s')J_z(l')\,dl'. \tag{9b}$$

It is pointed out that, in deriving (8a) and (9a), we divided both sides by k: this is permitted because any of its possible values (eigenvalues to be determined) must be different from zero either for TE or TM modes.

III. Procedure for the Calculation of TE Modes

J_t is represented as

$$J_t(l') = \sum_{n=1}^{N} b_n w_n(l') \tag{10}$$

where $\boldsymbol{b} = (b_1, b_2, \cdots, b_N)$ is an N-dimensional vector of numerical coefficients and $\{w\}$ is an N-dimensional set of base functions defined on σ.

The infinite summation in (8a) is truncated up to the Mth term, that is equivalent to truncate the series in the Green's function (3): this is a good approximation provided k is sufficiently smaller than k_M.

For computing purposes, σ is divided into N elements, each being approximated by a segment. The lengths of the segments may differ from each other. Functions w_n may be chosen as shown in Fig. 2 where, for ease of representation, σ has been drawn as a straight line. Functions w_n are piece-wise parabolic and their derivatives are piece-wise linear. Functions like the one sketched in Fig. 2(a), defined on three consecutive segments, are used when both extrema neither belong to the boundary of S_0 nor are edge points. Functions like those sketched in Fig. 2(b) and (c), defined on two consecutive segments only, are used when one extremum lies on the boundary of S_0 or is an edge point. The choice of these latter functions accounts for the features of the current at these particular points, namely: a) the current may differ from zero at the extrema of σ that belong to the boundary of S_0, but its derivative must be zero thereat; b) the current must be zero at the edges but its derivative may differ from zero (theoretically, of course, it is either zero or it diverges). Base functions with derivative diverging at edges might be considered if an improved approximation for the current is desired. Functions w_n are interlaced as shown in Fig. 2(d) and they permit to synthesize very good approximations for the current.

Substituting (10) into (8a) and (8b) and using Galerkin's procedure [11] we obtain the following algebraic eigenvalue problem:

$$\left\{ \begin{bmatrix} \boldsymbol{U} & \boldsymbol{O}_t \\ \boldsymbol{O} & \boldsymbol{C} \end{bmatrix} - k^2 \begin{bmatrix} \boldsymbol{D} & \boldsymbol{R}_t \\ \boldsymbol{R} & \boldsymbol{L} \end{bmatrix} \right\} \begin{bmatrix} \boldsymbol{a} \\ \boldsymbol{b} \end{bmatrix} = 0 \tag{11}$$

where $\boldsymbol{a} = (a_1, a_2, \cdots, a_M)$, $\boldsymbol{U}$ is the unit matrix of order M, $\boldsymbol{O}$ is the $N \times M$ null matrix, the subscript t denotes the transpose and

$$\boldsymbol{D} = \operatorname{diag}\left(k_1^{-2}, k_2^{-2}, \cdots, k_M^{-2}\right) \tag{12a}$$

$$C_{ij} = \int_\sigma \int_\sigma g(\boldsymbol{s}, \boldsymbol{s}') \frac{\partial w_i(l)}{\partial l} \frac{\partial w_j(l')}{\partial l'} \, dl \, dl' \tag{12b}$$

$$L_{ij} = \int_\sigma \int_\sigma w_i(l) w_j(l') \boldsymbol{t}(l) \cdot \bar{\boldsymbol{G}}_{st}(\boldsymbol{s}, \boldsymbol{s}') \cdot \boldsymbol{t}(l') \, dl \, dl' \tag{12c}$$

$$R_{im} = \frac{1}{k_m^2} \int_\sigma w_i(l) \boldsymbol{t}(l) \cdot \boldsymbol{e}_m(\boldsymbol{s}) \, dl \tag{12d}$$

$$i, j = 1, 2, \cdots, N \qquad m = 1, 2, \cdots, M.$$

When determining (12b) we again used integration by parts and took into account that either g or w_n vanish at the extrema of σ.

Matrices $\boldsymbol{C}$ and $\boldsymbol{L}$ are symmetric because of the reciprocity properties of $\bar{\boldsymbol{G}}_{st}$ and g. In cases when σ is either a loop-shaped line or a line connecting two points belonging to the boundary of S_0, our functions w_n permit one to synthesize constant currents. This implies that, in these cases, a linear combination of the derivatives of the functions w_n exists which vanishes on σ. Then, in the said cases, the derivatives of the functions w_n, unlike the functions themselves, are not independent of each other. This observation is important in view of the considerations reported in Appendix II which lead to conclude that: a) matrix $\boldsymbol{L}$ is always positive definite; b) matrix $\boldsymbol{C}$ is positive definite only when σ (or any portion of it) is an open line not connecting points lying on the boundary of S_0; c) otherwise $\boldsymbol{C}$ is only semipositive definite and its rank is $R = N - P$ where P is the number of loops of σ plus the parts of σ connecting points belonging to the boundary of S_0. In the last case P, vectors $\boldsymbol{b}$ exist such that $\boldsymbol{Cb} = 0$: it is evident by inspection that such vectors associated with a null vector $\boldsymbol{a}$ satisfy (7) with the eigenvalue $k = 0$. This type of solution must be rejected as spurious.

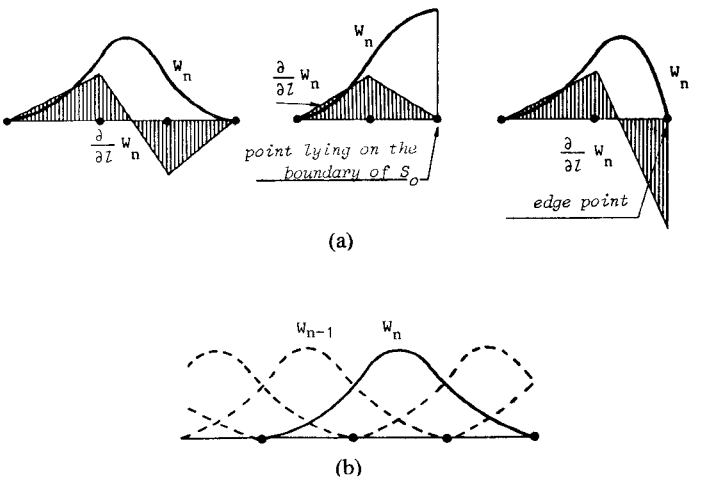

Fig. 2. Piece-wise parabolic base functions used for representing the transverse current on the sheet and their derivatives.

The solution of (11) constitutes a linear matrix eigenvalue problem of order $M + N$, which can be solved using library-routines such as those described in [12]. A more specialized algorithm based upon the semipositive definiteness of matrix $\boldsymbol{C}$ and the positive definiteness of matrix $\boldsymbol{L}$ may be used [13]. This algorithm reduces (11) to a standard matrix eigenvalue problem ($\boldsymbol{Ax} = \lambda \boldsymbol{x}$) of order $M + R$, and calculates only the meaningful (positive) eigenvalues.

Some doubts could probably arise about the validity of this procedure when σ happens to be everywhere perpendicular to the electric field of one of the modes of the unperturbed waveguide, say the mth one: in fact, that mode pertains to the perturbed waveguide as well and its cutoff wavenumber k_m must be an eigenvalue of (11), so that (8b) becomes indeterminate because $\boldsymbol{e}_m \cdot \boldsymbol{t} = 0$ and $k = k_m$. However, since $R_{im} = 0$ for every i (see (12d)), it turns out that the only equation in system (11) containing a_m is the mth one, namely

$$a_m\left(1 - k^2/k_m^2\right) = 0.$$

Then it is evident that a solution of (11) exists such that $k = k_m$, $a_m \neq 0$, with all the other variables equal to zero. This is exactly what is expected, so that our procedure holds also in this particular case.

The field distribution pertaining to any value of k thus found may be calculated using the expression

$$\boldsymbol{E}_t(\boldsymbol{r}) = -j\eta \left\{ \sum_{n=1}^{N} b_n \left[\frac{1}{k} \nabla \int_\sigma g(\boldsymbol{r}, \boldsymbol{s}') \frac{\partial w_n(l')}{\partial l'} \, dl' + k \int_\sigma \bar{\boldsymbol{G}}_{st}(\boldsymbol{r}, \boldsymbol{s}') \cdot \boldsymbol{t}(l') w_n(l') \, dl' \right] + k \sum_{m+1}^{M} \frac{a_m \boldsymbol{e}_m(\boldsymbol{r})}{k_m^2} \right\}. \tag{13}$$

In cases when σ divides S_0 into two or several separate parts, the calculation of $\boldsymbol{E}$ at some points suitably placed inside them permits one to understand whether a cutoff wavenumber pertains to the region of interest: in this case, indeed, the field in this region strongly exceeds that in the remaining regions, which is nearly zero. In some cases, however, the dimensions of the interesting portion of S_0 are much larger than those of the other portions so that one can expect that the lower eigenvalues pertain to the region of interest. In these cases, the said test procedure might be omitted.

IV. Procedure for the Calculation of TM Modes

In comparison with the aforesaid procedure, the determination of TM modes is fairly easier because (9a) is simpler than (8). J_z is represented as

$$J_z(l') = \sum_{n=1}^{N} b'_n u_n(l') \tag{14}$$

where $\boldsymbol{b}' = (b'_1, b'_2, \cdots, b'_N)$ is an N-dimensional vector of numerical coefficients and $\{u\}$ is an N-dimensional set of base functions defined on σ. Triangular functions as those shown in Fig. 3 may be chosen. When edge points are present, "half-triangle" base functions are considered (Fig. 3(b)) in order to approximate the possible singularity in J_z. When an improved approximation of the current is desired, singular base functions might be considered. Applying Galerkin's method, the problem is cast into the matrix form

$$\left\{ \begin{bmatrix} \boldsymbol{U} & \boldsymbol{O}_t \\ \boldsymbol{O} & \boldsymbol{O}' \end{bmatrix} - k^2 \begin{bmatrix} \boldsymbol{D}' & \boldsymbol{R}'_t \\ \boldsymbol{R}' & \boldsymbol{L}' \end{bmatrix} \right\} \begin{bmatrix} \boldsymbol{a}' \\ \boldsymbol{b}' \end{bmatrix} = 0 \tag{15}$$

where $\boldsymbol{a}' = (a'_1, a'_2, \cdots, a'_M)$, $\boldsymbol{O}'$ is the $N \times N$ null matrix and

$$\boldsymbol{D}' = \operatorname{diag}\left(k_1'^{-2}, k_2'^{-2}, \cdots, k_M'^{-2}\right) \tag{16a}$$

$$L'_{ij} = \int_\sigma \int_\sigma u_i(l)\, g(s,s')\, u_j(l')\, dl\, dl' \tag{16b}$$

$$R'_{im} = \frac{1}{k_m'^2} \int_\sigma u_i(l)\, \psi_m(s)\, dl. \tag{16c}$$

Evidently problem (15) admits N independent solutions with $k = 0, \boldsymbol{a}' = 0, \boldsymbol{b}' \neq 0$, which must be discarded. Anyway, problem (15) may be easily cast into the standard form

$$\left(\boldsymbol{D}' - \boldsymbol{R}'_t \boldsymbol{L}'^{-1} \boldsymbol{R}\right) \boldsymbol{a}' = k^{-2} \boldsymbol{a}' \tag{17}$$

which admits only M eigenvalues and eigenvectors. Vector $\boldsymbol{b}'$ is deduced from $\boldsymbol{a}'$ by

$$\boldsymbol{b}' = -\boldsymbol{L}'^{-1} \boldsymbol{R}' \boldsymbol{a}'. \tag{18}$$

The rearrangement of (15) into (17) and (18) is possible because $\boldsymbol{L}'$ is always nonsingular (see Appendix II). Also for TM modes, it is easily shown that no problem arises in particular cases when σ does not perturb a certain waveguide mode, that is when ψ_m is everywhere zero on σ.

The field is calculated using

$$E_z(\boldsymbol{r}) = -j\eta k \left[\sum_{n=1}^{N} b'_n \int_\sigma g(\boldsymbol{r}, s')\, u_n(l')\, dl' + \sum_{m+1}^{M} k_m'^{-2} \psi_m(\boldsymbol{r})\, a'_m \right]. \tag{19}$$

In cases when σ divides S_0 into separate regions, the identification of the modes pertaining to the region of interest is done following the same procedure described for TE modes.

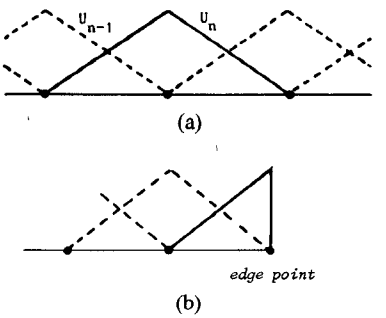

Fig. 3. Triangular base functions used for representing the longitudinal current on the sheet (or the charge, in the case of TEM modes).

V. Procedure for the Calculation of TEM Modes

This case, included for completeness, is totally independent of the above considerations. In fact, here one is interested only in modal fields, because cutoff wavenumbers are obviously zero. These fields are determined as gradients of the electrostatic potential $\Phi(\boldsymbol{r})$, which may be expressed using the same scalar Green's function g previously considered. We have

$$\Phi(\boldsymbol{r}) = \int_\sigma g(\boldsymbol{r}, s')\, \rho_\sigma(l')\, dl' \tag{20}$$

where ρ_σ represents the surface charge density on σ.

Let us consider the case where Q inner conductors exist, whose contours are the separate lines $\sigma_1, \sigma_2, \cdots, \sigma_Q$, not contacting the boundary of S_0. In this case, σ is constituted by the set of the said lines and, perhaps, by a further separate line σ^* contacting the boundary of S_0.

For any of the Q basic TEM modes, $\Phi(\boldsymbol{r})$ is uniquely determined by assigning the potentials $\Phi_1, \Phi_2, \cdots, \Phi_Q$ at the inner conductors [15]. Denoting with u_n triangular base functions like those shown in Fig. 3, the charge density inside S_0 may be represented as

$$\rho_\sigma(l') = \sum_{n=1}^{N^*} b''_n u_n(l') + \sum_{n=N^*+1}^{N^*+N_1} b''_n u_n(l') + \cdots + \sum_{m=N-N_Q+1}^{N} b''_n u_n(l') \tag{21}$$

where each summation represents the charge distribution on the various separate portions of σ, and $N^*, N_1, \cdots, N_Q$ are the numbers of the base functions on $\sigma^*, \sigma_1, \cdots, \sigma_Q$.

Observing that the potential on σ^* must be zero like the potential of the boundary of S_0, Galerkin's procedure yields

$$\boldsymbol{L}' \boldsymbol{b}'' = \boldsymbol{f} \tag{22}$$

where $\boldsymbol{b}''$ is the N-dimensional vector constituted by coefficients b''_n, L' is the same $N \times N$ matrix defined by (16b), and $\boldsymbol{f}$ is the N-dimensional vector defined as

$$f_n = \begin{cases} 0, & \text{for } 1 \leqslant n \leqslant N^* \\ \Psi_q \displaystyle\int_{\sigma_q} u_n(l')\, dl' & \text{for } N^* + \cdots + N_{q-1} < n \\ & \leqslant N^* + \cdots + N_{q-1} + N_q. \end{cases}$$

Since $\boldsymbol{L}'$ is nonsingular, system (21) yields a solution for any given vector $\boldsymbol{f}$.

The expression for calculating $\Phi(\boldsymbol{r})$ is

$$\Phi(\boldsymbol{r}) = \sum_{n=1}^{N} b'' \int_\sigma g(\boldsymbol{r}, s')\, u_n(l')\, dl'. \tag{23}$$

VI. Outline of the Method for Computing Matrix Elements

A program has been set up which follows the discussed procedure. Here we limit ourselves to outline the method adopted for computing matrix elements but we fail to discuss specific questions (for instance, the possibility of reducing the size of the matrices when symmetric geometries are dealt with, etc.). More details may be found in [13].

Let us consider, for instance, the coefficient L'_{ij} given by (16b). Due to the singular behavior of g, it is convenient to split g into a singular and a regular part, writing

$$g(s,s') = -\frac{1}{2\pi}\ln R + g_0(s,s')$$

where $R = |s - s'|$ and g_0 is a regular function deducible from the expressions reported in Appendix I. Then L'_{ij} may be cast into the form

$$L'_{ij} = \int_{\Delta_i} u_i(l)\, x_j(l)\, dl + \int_{\Delta_i} u_i(l)\, y_j(l)\, dl \qquad (24)$$

where

$$x_j(l) = -\frac{1}{2\pi}\int_{\Delta_j} u_j(l')\ln R\, dl' \qquad (25a)$$

$$y_j(l) = \int_{\Delta_j} u_j(l')\, g_0(s,s')\, dl' \qquad (25b)$$

and Δ_i denotes the support of the function u_i.

It is noted that functions x_j and y_j are regular and that function x_j may be calculated analytically. Anyway, functions x_j and y_j exhibit a quite complicated behavior which discourages the exact analytical calculation of L'_{ij}. For this reason, the integrations appearing in (24) are performed analytically using piece-wise parabolic approximations of these functions in place of their exact expressions. The coefficients appearing in the parabolic approximations are calculated in such a way that the approximate functions are coincident with the exact values at three points within each segment constituting Δ_i. Then the computation of the integrals in (24) requires the previous determination of the functions x_j and y_j at six points (or three points in case of Δ_j placed at an edge , see Fig. 3(b)). The values of x_j are directly obtained from the known expression of this function whereas the values of y_j are computed from (25b) using similar piece-wise parabolic approximations for g_0.

The computation of coefficients C_{ij}, L_{ij}, which involves singular integrands like the one discussed above, is performed following the same procedure. The calculation of coefficients R_{im}, R'_{im}, is carried out using parabolic approximations for the functions $t(l)\cdot e_m(s)$ and $\psi_m(s)$.

It is pointed out that this method of computation is much faster than conventional numerical integration; furthermore, our choice of a parabolic approximation of the functions to be integrated allows a high accuracy even in cases when Δ_i and Δ_j are close to each other or when Δ_i and/or Δ_j are not small. This advantages overwhelm the algebraic complexity of the procedure we adopted.

VII. Some Examples

The first example refers to a circular waveguide perturbed by a radial conducting sheet (see Fig. 4). This example has been chosen because the theoretical solution is known, thus permitting the evaluation of the precision obtained. The sheet has been divided into four segments, the one at the edge being much shorter than the others, in order to achieve a good representation of the rapid variations of the current near the edge while using a base function of the type shown in Fig. 2(c). The errors in the cutoff frequencies obtained for the lower TE and TM modes are reported in Table I, together with CPU time and memory requirements referred to a Honeywell DPS8/44 computer (time for tracing the mode patterns is not included). Fig. 4 shows the mode patterns. TE mode patterns refer to the electric field, as calculated using (13). TM mode patterns represent the magnetic-field lines obtained as constant-E_z contours. E_z was calculated using (19).

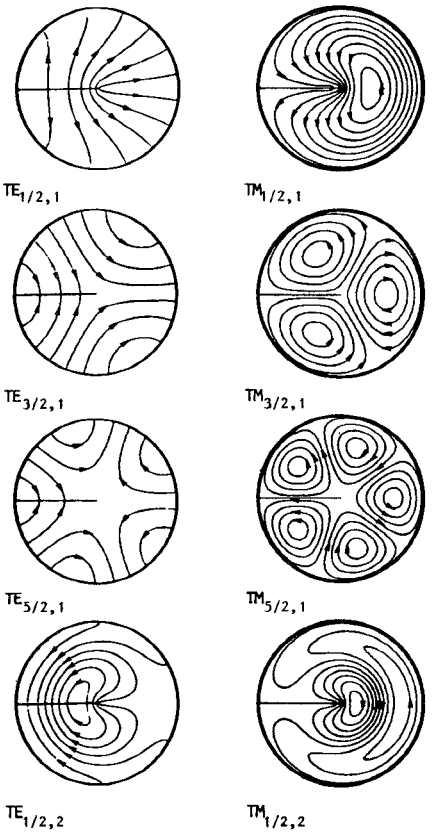

Fig. 4. Calculated mode patterns for a circular waveguide perturbed by a radial fin. TE and TM mode patterns show the electric and magnetic field-lines, respectively.

TABLE I

MODE	ERROR (%)	N	M	CPU TIME	MEMORY
$TE_{1/2,1}$	0.3 (0.1)	4	4	10 SEC	22 K
$TE_{3/2,1}$	0.3 (0.2)				
$TE_{5/2,1}$	0.7 (0.7)				
$TE_{1/2,2}$	5.1 (5.1)				
$TM_{1/2,1}$	0.02	5	9	14 SEC	24 K
$TM_{3/2,1}$	0.06				
$TM_{5/2,1}$	0.10				
$TM_{1/2,2}$	0.24				

The accuracy obtained in the calculation of the field for the $TE_{1/2.1}$ mode is better illustrated in Fig. 5(a), which represents the electric field along the diameter containing the perturbing fin.

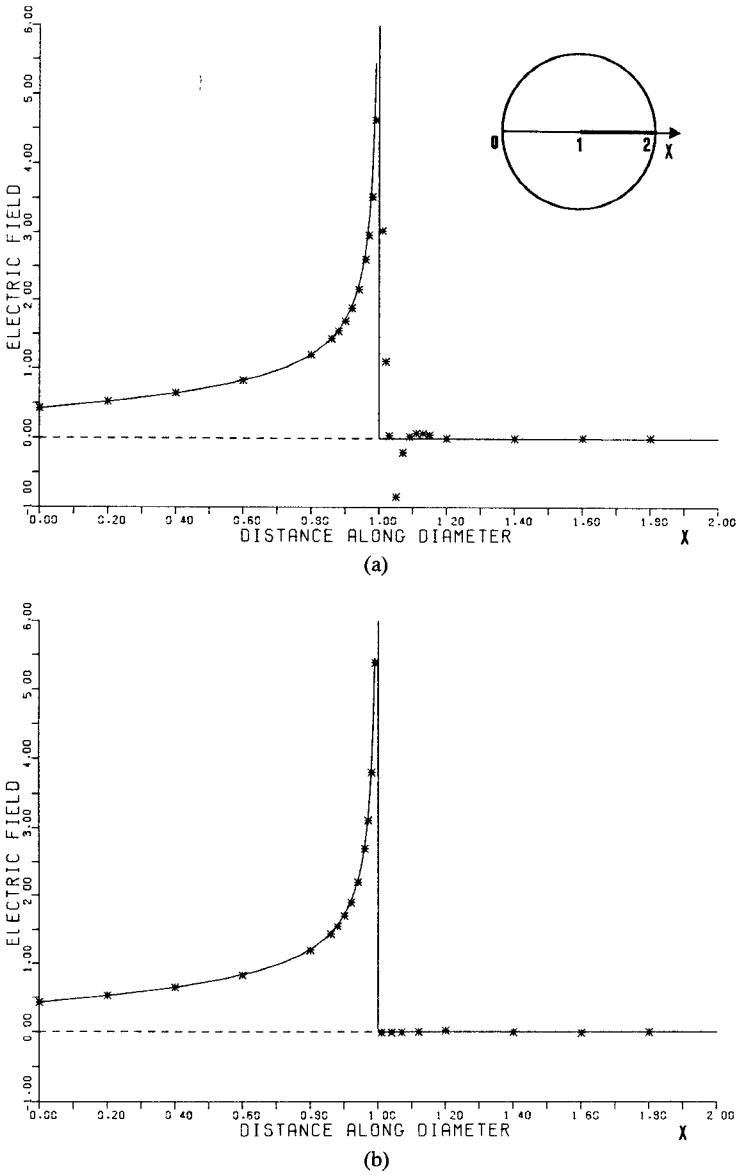

Fig. 5. Electric field along the diameter computed using: (a) base function with finite derivative at the edge, (b) base function with the correct diverging derivative at the edge.

Computed values (represented by stars) are very close to the theoretical ones (continuous line) except near to the tip of the perturbing conductor. Field errors are ascribed to the use of a base function having a finite derivative at the tip of the fin, which does not permit a sufficiently good approximation of the current, whose derivative should diverge like $(x-1)^{-1/2}$. It is noted, however, that the inaccuracy of the representation of the current has a small influence on the accuracy of the computed cutoff wavenumbers: for instance, in spite of the small values of N and M, the dominant cutoff wavenumber has an error of only 0.3 percent. This happens because the cutoff wavenumber is a variational quantity, whereas the field is not.

On the other hand, considering a more appropriate base function, whose derivative diverges with the correct law at the edge, is no problem and it only introduces a small complication. We explored the utility of introducing such a base function in the computation of TE modes. In this case, the fin has been subdivided into equal parts and the calculation has been repeated with the same values of N and M as before. We found even better precision in the calculation of the cutoff wavenumbers (see Table I, values in parentheses) and negligible field errors everywhere (see Fig. 5b).

The second example concerns the calculation of the TM modes for a circular waveguide starting from a square cross section. Mode patterns and accuracies in wavenumbers are represented in Fig. 6. This computation was performed considering the symmetry with respect to a median of the square. In this calculation, we employed $N=10, M=8$. It is pointed out that the computed fields were practically zero outside the region of interest. The obtained accuracy was very good.

Figs. 4–6 evidence the excellent representation of the field discontinuities at σ. This is a consequence of the use of a Green's function where the singularity is expressed in closed form.

The last example concerns the double-ridged waveguide studied by Jull *et al.* [14] and, more recently, by Dasgupta and Saha [3] (see Fig. 7). The values of λ_c/a obtained for the first two TE modes are reported in Table II. In this example, we used $N=11, M=3$ and we considered the symmetry.

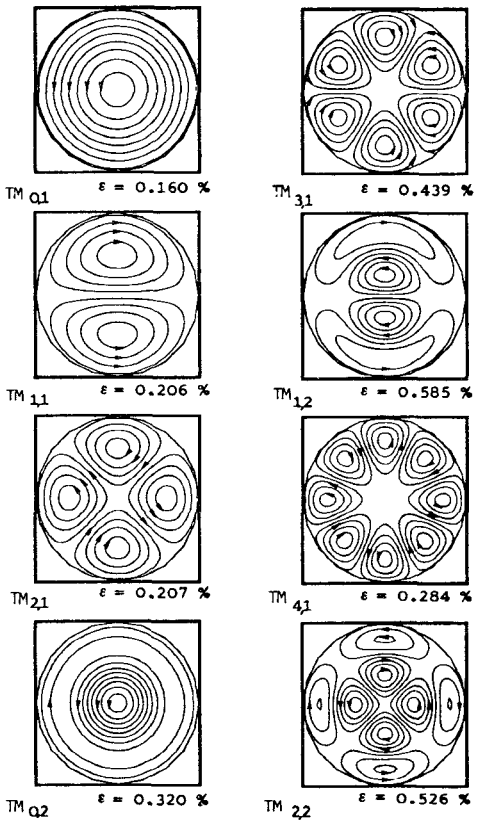

Fig. 6. Calculated TM mode patterns for the circular waveguide studied as a square waveguide perturbed by a tubular sheet. The quantity ϵ is the error percent of the calculated cutoff wavenumbers.

We note that our method is particularly well suited for studying the dominant mode of a reentrant waveguide as the one we considered. In fact, in this case, the first eigenvalue is much smaller than the cutoff wavenumber of the dominant mode for the unperturbed guide, so that the modal series may be truncated up to a very small number of terms (M equal 2, 1, or even 0!) without any significant loss of accuracy. In other words, in this case the field is determined very well using the low-frequency approximation of the Green's function.

VIII. Computational Advantages

Our method requires the solution of a linear eigenvalue problem of order $N+M$ or N for the determination of TE or TM modes, respectively. We recall that N is the number of the variables b, representing the current over the portion of the boundary not coincident with the rectangular or the circular boundary of S_0 and M is the number of the auxiliary variables a, introduced to reduce the eigenvalue problem into a linear form. Other methods based on an integral equation require the solution of a nonlinear eigenvalue problem of order $N' \geq N$, equal to the number of the variables needed to represent the current over the whole boundary of the waveguide. In this section, we compare the computation time required by our method with that required by other methods. In this comparison we refer to the computation of TE modes, which is more cumbersome than the computation of TM modes.

When most of the perturbed boundary coincides with the unperturbed rectangular or circular boundary, in spite of the introduction of the auxiliary variables a, $N+M$ may be less than N' and the computational advantage of using our method is evident. Some doubts might arise about the utility of our algorithm when the perturbed boundary is totally inside the unperturbed boundary, since in this case our integral equation is over the whole boundary as in other integral equation methods, and $N+M > N'$. Furthermore, our Green's function looks more complicated than the free-space Green's function usually employed in other methods.

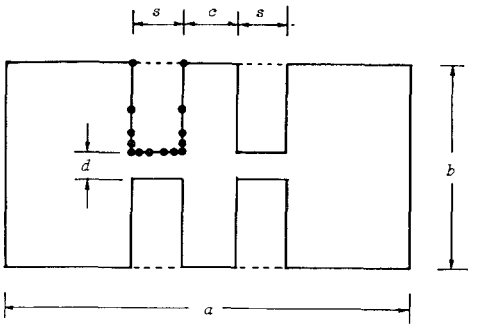

Fig. 7. Double-ridged waveguide. The relative dimensions are: $b/a = 0.5$; $d/b = s/a = c/a = 0.125$. The points drawn on a ridge indicate the subdivision adopted in the calculation.

TABLE II

MODE	OUR METHOD	JULL ET AL.	DASGUPTA SAHA
TE 1ST	4.549	4.47	4.516
TE 2ND	1.917	-	1.905

Let us consider a typical case where the unperturbed boundary is circular and $N=10$, $M=8$. We found experimentally that, in this case, CPU time required to perform the main operations is approximately subdivided as follows:

computation of matrix $\boldsymbol{C}(10\times10)$	0.2 T
computation of matrix $\boldsymbol{L}(10\times10)$	0.4 T
computation of matrix $\boldsymbol{R}(8\times10)$	0.1 T
solution of the eigenvalue problem	0.1 T

where T is the total CPU time. It turned out that about 8–10 of the computed modes were determined with acceptable accuracy.

Let us suppose to solve the same problem by the Spielman–Harrington method [7], which we assume as representative of other integral equation methods. Using this method, the cutoff wavenumbers should be determined as the values of k which minimize the determinant of a complex 10×10 matrix $\boldsymbol{Z}(k)$, whose elements are calculated using a formula similar to (12b), but involving, in place of g, a Hankel function of argument depending on k. We estimate that the calculation of $\boldsymbol{Z}(k)$ should require a time of the same order of the time needed to calculate our matrix $\boldsymbol{C}$, that is 0.2 T. Localizing any of the minima of $\det \boldsymbol{Z}(k)$ should require repeated calculations of the elements of $\boldsymbol{Z}(k)$ and of its determinant. Then, we may estimate that only five of these calculations should take a longer time than T and only five computations of $\det \boldsymbol{Z}(k)$ are by far insufficient to localize a minimum, especially when no estimate of its location is available. Furthermore, the determination of the wall current for any mode should require the computation of the eigenvector corresponding to the smallest eigenvalue of the matrix $\boldsymbol{X} = \operatorname{Im} \boldsymbol{Z}(\boldsymbol{k})$.

These brief considerations show the computational advantage of our method, especially when more than one mode is to be determined. It is pointed out that the advantage derives from the possibility of reducing the determination of the cutoff wavenumbers to the solution of a linear eigenvalue problem, where matrix elements are calculated only once.

APPENDIX I

A. Expressions of g and $\bar{G}_{st}$ for Two-Dimensional Resonators of Circular Cross Section

The radius of the circle is indicated by a and the polar coordinates of the observation and source point are indicated by r, ϕ; r', ϕ', respectively. Fundamental unit vectors at the observation and at the source point are indicated by $\hat{r}, \hat{\phi}, \hat{r}', \hat{\phi}'$. We have

$$g(r,\phi,r',\phi') = \frac{1}{2\pi}\ln(r'R_i/aR)$$

$$\begin{aligned}\bar{G}_{st}(r,\phi,r',\phi') = {} & \frac{\hat{r}\hat{r}'}{8\pi}\left[2C\ln(r'R_i/aR) + \frac{(r^2+r'^2)C-2rr'}{R^2} + \frac{(r^2+r'^2+4a^2)C-2rr'}{(r'R_i/a)^2}\right.\\ & \left. -\left(1+\frac{a^2}{r^2}\right)\left(1+\frac{a^2}{r'^2}\right)\left(LC-AS+\frac{rr'}{(r'R_i/a)^2}\right)\right]\\ & + \frac{\hat{\phi}\hat{r}'}{8\pi}\left[-2S\ln(r'R_i/aR) + \frac{(r^2-r'^2)S}{R^2} + \frac{(r^2+r'^2-2a^2)S}{(r'R_i/a)^2} + \left(1-\frac{a^2}{r^2}\right)\left(1+\frac{a^2}{r'^2}\right)(LS+AC)\right]\\ & + \frac{\hat{r}\hat{\phi}'}{8\pi}\left[2S\ln(r'R_i/aR) + \frac{(r^2-r'^2)S}{R^2} - \frac{(r^2+r'^2-2a^2)S}{(r'R_i/a)^2} - \left(1+\frac{a^2}{r^2}\right)\left(1-\frac{a^2}{r'^2}\right)(LS+AC)\right]\\ & + \frac{\hat{\phi}\hat{\phi}'}{8\pi}\left[2C\ln(r'R_i/aR) - \frac{(r^2+r'^2)C-2rr'}{R^2} + \frac{(r^2+r'^2-2a^2)(rr'/a^2-C)}{(r'R_i/a)^2} - \frac{rr'}{a^2}\right.\\ & \left. -\left(1-\frac{a^2}{r^2}\right)\left(1-\frac{a^2}{r'^2}\right)\left(LC-AS+\frac{rr'}{a^2}\right)\right].\end{aligned}$$

$$R = (r^2+r'^2-2rr'C)^{1/2}$$

$$R_i = (r^2+a^4/r'^2-2ra^2C/r')^{1/2}$$

$$C = \cos(\phi-\phi')$$

$$S = \sin(\phi-\phi')$$

$$L = \ln(r'R_i/a^2)$$

$$A = tg^{-1}[rr'S/(a^2-rr'C)].$$

B. Expressions of g and $\bar{G}_{st}$ for Two-Dimensional Resonators of Rectangular Cross Section

The section is referred to x, y axes with the origin placed at a corner. The length of the sides of the rectangle are indicated by a (in the x direction) and b. The fundamental unit vectors are indicated by $\hat{x}, \hat{y}$. We have the following expressions:

$$\begin{aligned}g(x,y,x',y') &= -\sum_{-\infty}^{\infty} m,n \frac{(-1)^{m+n}}{2\pi}\ln R_{mn}\\ &= \sum_{-\infty}^{\infty} m\frac{(-1)^m}{4\pi}\ln\frac{V_m-C}{V_m-A}\\ &= \sum_{-\infty}^{\infty} m\frac{(-1)^m}{4\pi}\ln\frac{T_m-D}{T_m-B}\end{aligned}$$

$$\begin{aligned}\bar{G}_{st}(x,y,x',y') &= \frac{\hat{x}\hat{x}}{4\pi}\sum_{-\infty}^{\infty} m\left[\frac{1}{2}\ln\frac{T_m-D}{T_m-B} + \frac{IMX_mS_m}{(T_m-B)(T_m-D)}\right]\\ &\quad - \frac{\hat{x}\hat{y}}{4\pi}\sum_{-\infty}^{\infty} m\frac{GY_m(V_mF-H)}{(V_m-A)(V_m-C)}\\ &\quad - \frac{\hat{y}\hat{x}}{4\pi}\sum_{-\infty}^{\infty} m\frac{MX_m(T_mL-N)}{(T_m-B)(T_m-D)}\\ &\quad + \frac{\hat{y}\hat{y}}{4\pi}\sum_{-\infty}^{\infty} m\left[\frac{1}{2}\ln\frac{V_m-C}{V_m-A} + \frac{EGY_mU_m}{(V_m-A)(V_m-C)}\right]\end{aligned}$$

$$A = \cos[\pi(x-x')/a]$$

$$B = \cos[\pi(y-y')/b]$$

$$C = \cos[\pi(x+x')/a]$$

$$D = \cos[\pi(y+y')/b]$$

$$E = \sin(\pi x/a)$$

$$F = \cos(\pi x/a)$$

$$G = \sin(\pi x'/a)$$

$$
\begin{aligned}
H &= \cos(\pi x'/a)\\
I &= \sin(\pi y/b)\\
L &= \cos(\pi y/b)\\
M &= \sin(\pi y'/b)\\
N &= \cos(\pi y'/b)\\
R_{mn} &= \left[(x-x_m)^2+(y-y_n)^2\right]^{1/2}\\
x_m &= (m+1/2)\,a+(-1)^m(x'-a/2)\\
y_m &= (m+1/2)\,b+(-1)^m(y'-b/2)\\
X_m &= \pi(x-x_m)/b\\
Y_m &= \pi(y-y_m)/a\\
S_m &= \sinh(X_m)\\
T_m &= \cosh(X_m)\\
U_m &= \sinh(Y_m)\\
V_m &= \cosh(Y_m).
\end{aligned}
$$

Singularities in g and $\bar{\bar{G}}_{st}$ are exhibited by the terms corresponding to $m=0, n=0$.

Appendix II

A. Semipositive Definiteness of Matrix C

Let us consider the quadratic form $\boldsymbol{x}_t\boldsymbol{C}\boldsymbol{x}$ where $\boldsymbol{x}$ is any real N-dimensional vector different from zero. Due to (12b) we have

$$\boldsymbol{x}_t\boldsymbol{C}\boldsymbol{x}=\sum_{i,j}x_i x_j C_{ij}=\int_\sigma \psi(l)\,\rho(l)\,dl \tag{A1}$$

where

$$\rho(l)=\sum_i x_i\frac{\partial w_i}{\partial l}$$

$$\psi(l)=\int_\sigma g(s,s')\,\rho(l')\,dl'.$$

Due to the meaning of g, $\psi(l)$ is coincident with the electrostatic potential on σ given by a charge density ρ distributed on σ itself. Then (A1) is coincident with the expression of the electrostatic energy of this charge and, therefore, it is nonnegative. Null values of $\boldsymbol{x}_t\boldsymbol{C}\boldsymbol{x}$ may occur only with a vector $\boldsymbol{x}$ such that $\rho(l)$ is zero, or, equivalently, such that $\sum x_i w_i=$ constant. Due to the choice of the basis $\{w_i\}$ such a vector exists if σ connects two points lying on the boundary of S_0 (see Section III). More generally, denoting by P the sum of the number of the portions of σ which connect points on the boundary plus the number of loops, P independent such vectors exist. Then $\boldsymbol{C}$ has P null eigenvalues and its rank is $R=N-P$.

B. Positive Definiteness of Matrix L'

It is easily deduced that a quadratic form assoicated with $\boldsymbol{L}'$ represents the electrostatic energy due to a charge density given by

$$\rho'(l)=\sum_i x_i u_i.$$

This cannot vanish, due to the independence of the functions u_i. Then, the quadratic form is always positive and matrix $\boldsymbol{L}'$ is positive-definite.

C. Positive Definiteness of Matrix L

Due to (12c), a generic quadratic form associated with $\boldsymbol{L}$ is

$$\boldsymbol{x}_t\boldsymbol{L}\boldsymbol{x}=\sum_{i,j}\int_\sigma\int_\sigma u_i\boldsymbol{t}(l)\cdot\bar{\bar{G}}_{st}(s,s')\cdot\boldsymbol{t}(l')\,u_j\,dl\,dl'. \tag{A2}$$

The solenoidal dyad $\bar{\bar{G}}_{st}$ may be expanded as

$$\bar{\bar{G}}_{st}(\boldsymbol{r},\boldsymbol{r}')=\sum_m\frac{\boldsymbol{e}_m(\boldsymbol{r})\,\boldsymbol{e}_m(\boldsymbol{r}')}{k_m^2}. \tag{A3}$$

This expansion is easily established starting from (5), taking into account that $\nabla\times\nabla\times\boldsymbol{e}_m=k_m^2\boldsymbol{e}_m$, $\boldsymbol{n}\times\boldsymbol{e}_m=0$ at the boundary, and using the property of eigenvectors $\boldsymbol{e}_m$ of being mutually orthogonal and orthogonal to $\nabla\nabla' g$. By substituting (A3) into (A2), we obtain

$$\boldsymbol{x}_t\boldsymbol{L}\boldsymbol{x}=\sum_m\left(\int_\sigma f(l)\frac{\boldsymbol{t}(l)\cdot\boldsymbol{e}_m(s)}{k_m}\,dl\right)^2$$

where $f(l)=\sum_1^N x_i w_i(l)$. Since functions w_i are linearly independent $f(l)$ cannot vanish, so that the quadratic form is always positive. Then matrix $\boldsymbol{L}$ is positive-definite.

References

[1] F. L. Ng, "Tabulation of methods for the numerical solution of the hollow waveguide problem," *IEEE Trans. Microwave Theory Tech.*, vol. MTT-22, no. 3, pp 322–329, Mar. 1974.

[2] P. Laura, L. Diez, C. Giannetti, L. E. Luisoni, and R. Grossi, "Calculation of the fundamental cutoff frequencies in a case of waveguide of doubly-connected cross section," *Proc. IEEE*, vol. 65, no. 9, pp. 1392–1395, Sept. 1977.

[3] D. Dasgupta and B. K. Saha, "Eigenvalue spectrum of rectangular waveguide with two symmetrically placed double ridges," *IEEE Trans. Microwave Theory Tech.*, vol. MTT-29, pp. 47–51, Jan. 1981.

[4] M. Ikeuchi, K. Inoue, H. Sawami, and H. Niki, "Arbitrarily shaped hollow waveguide analysis by the α-interpolation method," *SIAM, J. Appl. Math.*, vol. 40, no. 1, pp. 90–98, Feb. 1981.

[5] P. Saguet and E. Pic, "Le maillage rectangulaire et le changement de maille dans la methode TLM en deux dimensions," *Electron. Lett.*, vol. 17, no. 7, pp. 277–279, Apr. 1981.

[6] N. P. Malakshinov and A. S. Smagin, "Investigation of arbitrarily shaped regular waveguides by the method of auxiliary sources," *Radio Eng. Elec. Phys.*, vol. 27, June 1982, English transl. pp. 56–60.

[7] B. E. Spielman and R. F. Harrington, "Waveguide of arbitrary cross section by the solution of a non-linear integral eigenvalue equation," *IEEE Trans. Microwave Theory Tech.*, vol. MTT-20, no. 9, pp. 578–585, Sept. 1972.

[8] M. Bressan and G. Conciauro, "Rapidly converging expressions for dyadic Green's functions in two-dimensional resonators of circular and rectangular cross section," *Alta Frequen.* (special issue on Applied Electromagnetics), vol. 52, no. 3, pp. 188–190, 1983.

[9] N. Marcuvitz, *Waveguide Handbook*. Radiation Lab. MIT, Cambridge, MA, 1951, pp. 56–60, 66–70.

[10] A. D. Yaghjian, "Electric dyadic Green's functions in the source region," *Proc. IEEE*, vol. 28, no. 2, pp. 248–263, 1980.

[11] R. F. Harrington, *Field Computation by Moments Method*. New York: MacMillan, 1968.

[12] B. S. Garbow, J. M. Boyle, J. J. Dougarde, and C. B. Moler, "Matrix eigensystem routines—EISPACK guide extension," in *Lecture Notes in Computer Science*, no. 51, G. Goos and J. Hartmanis, Eds., Springer-Verlag, 1977.

[13] M. Bressan and C. Zuffada, "A computer program for studying TE modes in circular or rectangular waveguides strongly perturbed by axial cylindrical conductors," Dipartimento di Elettronica dell'Università di Pavia, Tech. Rep. RI-02/1983.

[14] E. V. Jull, W. J. Bleackley, and N. M. Steen, "The design of waveguides with symmetrically placed double ridges," *IEEE Trans. Microwave Theory Tech.*, vol. MTT-17, pp 397–399, Jul 1969.

[15] R. E. Collin, *Field Theory of Guided Waves*. New York: McGraw-Hill, 1960, pg. 124.

Correction to "Quasi-Optical Method for Measuring the Complex Permittivity of Materials"

F. I. SHIMABUKURO, MEMBER, IEEE

In the above paper,[1] in Column 1 of Table II on page 663, Reference [9] should read [10] and Reference [10] should read [12].

Manuscript received August 5, 1984.

[1] F. I. Shimabukuro *et al.*, *IEEE Trans. Microwave Theory Tech.*, vol. MTT-32, pp. 659–665, July 1984.

The author is with the Electronics Research Laboratory, Laboratory Operations, The Aerospace Corporation, El Segundo, CA 90245.